

AD \_\_\_\_\_

Award Number: W81XWH-09-1-0609

TITLE: Acquisition of High Field Nuclear Magnetic Resonance Spectrometers for Research in Molecular Structure, Function and Dynamics

PRINCIPAL INVESTIGATOR: George Pack

CONTRACTING ORGANIZATION: University of Louisville  
Louisville, KY 40208

REPORT DATE: September 2011

TYPE OF REPORT: Annual

PREPARED FOR: U.S. Army Medical Research and Materiel Command  
Fort Detrick, Maryland 21702-5012

DISTRIBUTION STATEMENT: Approved for public release; distribution unlimited

The views, opinions and/or findings contained in this report are those of the author(s) and should not be construed as an official Department of the Army position, policy or decision unless so designated by other documentation.

REPORT DOCUMENTATION PAGE				Form Approved OMB No. 0704-0188	
Public reporting burden for this collection of information is estimated to average 1 hour per response, including the time for reviewing instructions, searching existing data sources, gathering and maintaining the data needed, and completing and reviewing this collection of information. Send comments regarding this burden estimate or any other aspect of this collection of information, including suggestions for reducing this burden to Department of Defense, Washington Headquarters Services, Directorate for Information Operations and Reports (0704-0188), 1215 Jefferson Davis Highway, Suite 1204, Arlington, VA 22202-4302. Respondents should be aware that notwithstanding any other provision of law, no person shall be subject to any penalty for failing to comply with a collection of information if it does not display a currently valid OMB control number. <b>PLEASE DO NOT RETURN YOUR FORM TO THE ABOVE ADDRESS.</b>					
1. REPORT DATE (DD-MM-YYYY) 01-09-2011		2. REPORT TYPE Annual		3. DATES COVERED (From - To) 10 AUG 2010 - 9 AUG 2011	
4. TITLE AND SUBTITLE Acquisition of High Field Nuclear Magnetic Resonance Spectrometers for Research in Molecular Structure, Function and Dynamics				5a. CONTRACT NUMBER	
				5b. GRANT NUMBER W81XWH-09-1-0609	
				5c. PROGRAM ELEMENT NUMBER	
6. AUTHOR(S) George Pack  E-Mail: George.Pack@louisville.edu				5d. PROJECT NUMBER	
				5e. TASK NUMBER	
				5f. WORK UNIT NUMBER	
7. PERFORMING ORGANIZATION NAME(S) AND ADDRESS(ES) University of Louisville Louisville, KY 40208				8. PERFORMING ORGANIZATION REPORT NUMBER	
9. SPONSORING / MONITORING AGENCY NAME(S) AND ADDRESS(ES) U.S. Army Medical Research and Materiel Command Fort Detrick, Maryland 21702-5012				10. SPONSOR/MONITOR'S ACRONYM(S)	
				11. SPONSOR/MONITOR'S REPORT NUMBER(S)	
12. DISTRIBUTION / AVAILABILITY STATEMENT Approved for Public Release; Distribution Unlimited					
13. SUPPLEMENTARY NOTES					
14. ABSTRACT Two High-Field NMR spectrometers supported four research projects: Task 1, Mechanism of conversion of uridine to pseudouridine and to 4-thiouridine. We overexpressed the active C-terminal domain of enzyme Thil, required for 4-thiouridine modification of tRNA. The two pseudouridine synthetases, TruB and RluA convert uridine to pseudourine in tRNA. We show the two enzymes generate the same products of F5U. Task 2, Devising new nanocomposites that can enhance wound healing. We synthesized MgO nanoparticles and characterized their interactions with ATP. Task 3. Characterization of the complex between Factor XIII and fibrinogen in blood clotting. We have set up the expression system for Fbg αC 242-424 in Ecoli. A system that will subsequently be used to purify the expressed protein has been established. Task 4. NMR probes for elastin spectroscopy built and tested. An expression system for heterodimeric collagen has been established. The entropy of water molecules on the surface of elastin has been measured.					
15. SUBJECT TERMS modification; nanocomposites for wound healing; factor XIII in blood clots; tensile properties of proteins					
16. SECURITY CLASSIFICATION OF:			17. LIMITATION OF ABSTRACT	18. NUMBER OF PAGES	19a. NAME OF RESPONSIBLE PERSON
a. REPORT U	b. ABSTRACT U	c. THIS PAGE U			USAMRMC
			UU	18	19b. TELEPHONE NUMBER (include area code)

## Table of Contents

	<u>Page</u>
Introduction.....	4
Body.....	5
Key Research Accomplishments.....	14
Reportable Outcomes.....	15
Conclusion.....	16
References.....	17
Appendices.....	18

## **APPROVED SOW:**

### **Task 1. Mechanism of conversion of uridine to pseudouridine and to 4-thiouridine (Dr. E. G. Mueller).**

Year 1. Express unlabeled and carbon-13 and nitrogen-15 labeled C-terminal domain and begin acquiring and assigning spectra.

Year 2. Finish acquiring and assigning spectra; begin using distant constraints to establish the structure.

Year 3. Finish the structural determination; dock the C-terminal domain with the threaded N-terminal domain model.

### **Task 2. Devising new nanocomposites that can enhance wound healing (Dr. M. C. Yappert).**

Year 1. Synthesize magnesia nanoparticles that effectively bind ATP and other polar compounds.

- a. Sequential preparation of MgO/ATP nanocomposites.
- b. Characterize the interactions between MgO nanoparticles and ATP.

### **Task 3. Characterization of the complex between Factor XIII and fibrinogen (Dr. M. C. Maurer).**

Year 1. *E. coli* systems for expressing and purifying \_C 242-424 will be optimized for producing the large amounts of isotopically labeled protein needed for NMR studies. We anticipate that both wild type and selected mutants will be desired for the studies. Unlabeled recombinant wild type FXIII A2 and human derived FXIII B2 will also be collected. Assessing NMR chemical shift assignments will begin.

Year 2. The structural features of the \_C 242-424 segments will be determined and the sites of contact and reactivity with FXIII A2 and B2 will be started.

Year 3. Examine the dynamic properties of the \_C 242-424 system.

### **d. Tensile properties of fibrous proteins (Dr. R. J. Wittebort)**

Year 1: Complete <sup>13</sup>C, <sup>2</sup>H and <sup>17</sup>O NMR of elastin to test hypothesis I. Publish results on elastin's mechanism of elasticity. Express and purify collagen constructs.

## PROGRESS AGAINST APPROVED SOW:

### Task 1 Mechanism of conversion of uridine to pseudouridine and to 4-thiouridine (Dr. E. G. Mueller).

Year 1. Express unlabeled and carbon-13 and nitrogen-15 labeled C-terminal domain and begin acquiring and assigning spectra.

The overexpression of the C-terminal domain of ThiI in minimal medium and its subsequent purification have been successfully carried out using an established protocol.<sup>1</sup> After 4 h induction, the bacteria were pelleted, resuspended, and lysed. The lysate was subjected to purification over a “nickel column”, and the His<sub>6</sub>-tagged C-terminal domain of ThiI was eluted with buffer containing imidazole (250 mM) and collected in two fractions. SDS-PAGE analysis (Figure 1) revealed that even though an obvious band was observed during induction (lanes A-E), the C-terminal domain was obtained in reasonable purity and yield: 5.38 mg (400 nmol) from 500 mL culture.

Even allowing for a modest decrease in total yield during a “polishing” step of protein purification, these results establish the practicality of producing sufficient quantities of C-terminal domain in minimal medium for NMR studies. With the 700 MHz spectrometer now functional, the time is ripe to move forward with the production of labeled protein and data acquisition.

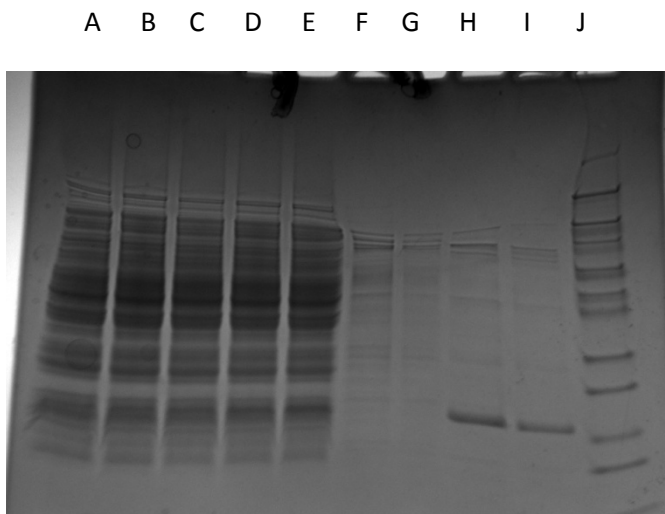


**Figure 1.** SDS-PAGE analysis of the induction (A-E) and purification (F-I) of the His<sub>6</sub>-tagged C-terminal domain of ThiI. Samples of total protein prepared from aliquots of the overexpression culture were loaded onto a gradient (4-20%) gel in volumes normalized for cell density and run using tricine (rather than glycine) in the anode buffer, which effects better resolution of small proteins. A, just before induction; B-E, 1 h, 2 h, 3 h, and 4h after induction, respectively. F-G, the first and second washes of the loaded Ni-NTA (Novagen) column; H-I, the first and second elution fractions showing the expected band (13.3 kDa) for the His<sub>6</sub>-tagged C-terminal domain. J, molecular weight markers.

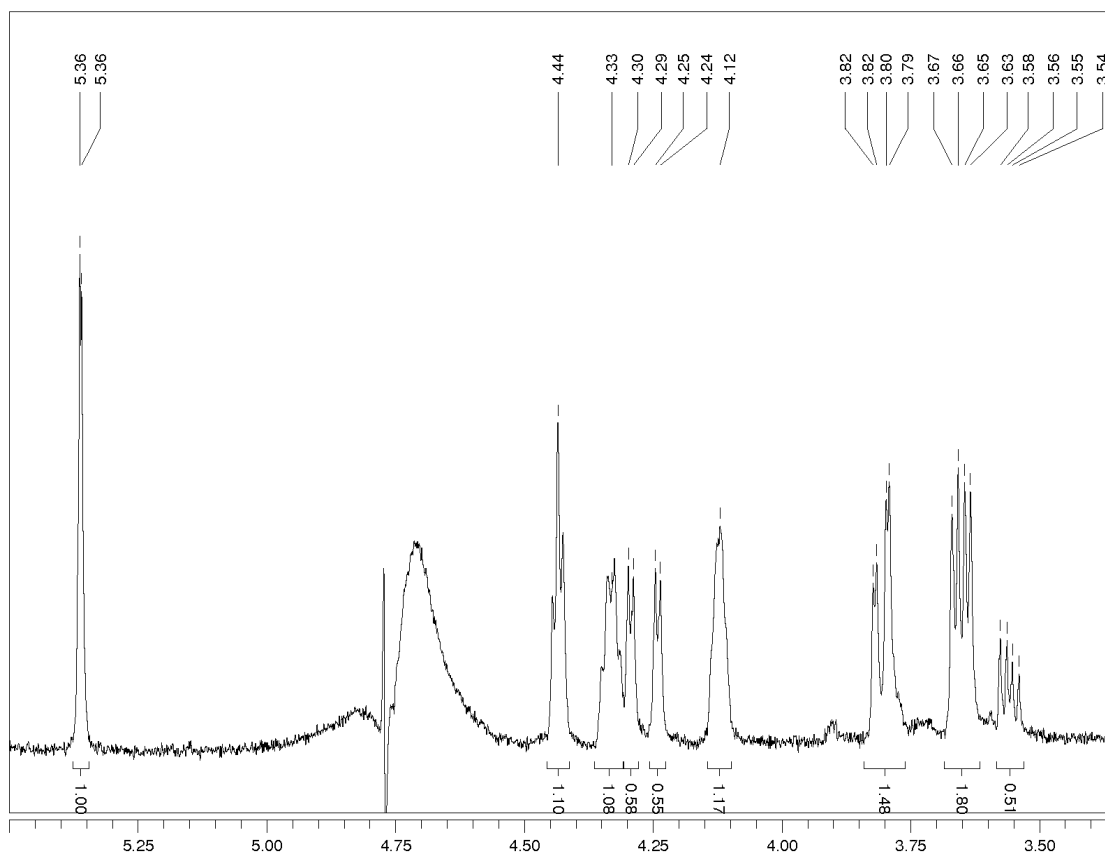
<sup>1</sup>Marley, J., Lu, M and Bracken, C. *J. Biomol. NMR*, **2001**, 20, 71-75.

*The degradation of the 3'-nucleoside of a dinucleotide.*

Two products of  $F^5U$  after the action of TruB were partially resolved by HPLC, and NMR characterization of the mixture of the products revealed that they were dinucleotides rather than the expected nucleosides because S1 nuclease does not cleave after nucleosides with nonplanar bases such as the hydrated, rearranged products of  $F^5U$ . The two products could conceivably be distinct conformers that interconvert only slowly rather than discrete stereoisomers, so it was proposed to remove the 3' nucleoside by cleaving it with periodate and subsequent elimination of the remnants by base treatment. The method proceeded well with two model dinucleotides and then was carried out on the mixture of dinucleotide products of  $F^5U$  from the action of TruB.

*The acquisition of spectral data for the [mononucleotide] product(s) of  $F^5U$*

The spectrum of the resulting mononucleotide product(s) (Figure 2) was very similar to that of the major product of  $F^5U$  in the dinucleotide. As foreseen, the periodate cleavage/base treatment/ion exchange purification led to the loss of approximately half of the sample on a molar basis (which is roughly 75% of the NMR signal since one half of the original dinucleotide products was degraded), so the signal to noise ratio of the spectrum falls well short of ideal. Additionally, the yield also leaves it uncertain whether or not periodate cleavage itself caused the disappearance of the minor product (which would argue for the two products being constrained conformers or for the peculiar susceptibility of the minor isomer to periodate or base treatment) or whether the level of sample loss resulted in an undetectably small amount of the minor product. The sample will be re-run on the 700 MHz instrument to benefit from its greater sensitivity in looking for a small percentage of a mononucleotide product corresponding to the minor dinucleotide product, for such an observation would make it much less likely that the two dinucleotide products are constrained conformers.



*The acquisition of spectral data for the dinucleotide product(s) of  $F^5U$  from the action of RluA on stem-loop  $[F^5U]RNA$ .*

**Figure 2.** The  $^1\text{H}$  NMR spectrum of the mononucleotide product resulting from the periodate cleavage/base treatment/anion exchange chromatography of the dinucleotide products of  $\text{F}^{5'}\text{U}$  from the action of TruB.

It was feared that the greater sensitivity of the 700 MHz would also be required to acquire suitable spectra of the products of  $\text{F}^{5'}\text{U}$  from the action of RluA since this enzyme forms a stoichiometric adduct with the  $[\text{F}^{5'}\text{U}]\text{RNA}$  so that the products would have to be purified away from a full equivalent of protein (rather than a catalytic amount of TruB, which treats  $[\text{F}^{5'}\text{U}]\text{RNA}$  as a substrate and achieves multiple turnovers). Happily, however, the technical difficulties in obtaining sufficient quantities of the product(s) of  $\text{F}^{5'}\text{U}$  after the action of RluA were not insurmountable, and sufficient quantities of products were obtained to acquire high quality spectra.

The 1D spectrum afforded a surprise. Even though only a single product peak is detected by  $\text{C}_{18}$  HPLC, the NMR spectrum of that peak showed that it contained two products of  $\text{F}^{5'}\text{U}$  with very similar spectra to the major and minor products obtained by the action of TruB (Figure 3). The most salient (yet trivial) differences arise from the identity of the 3' nucleoside in the dinucleotide products, which is C for the “TruB products” and U for the “RluA products” (because of the sequences of the stem-loop RNAs); the HPLC column simply does not resolve the latter.

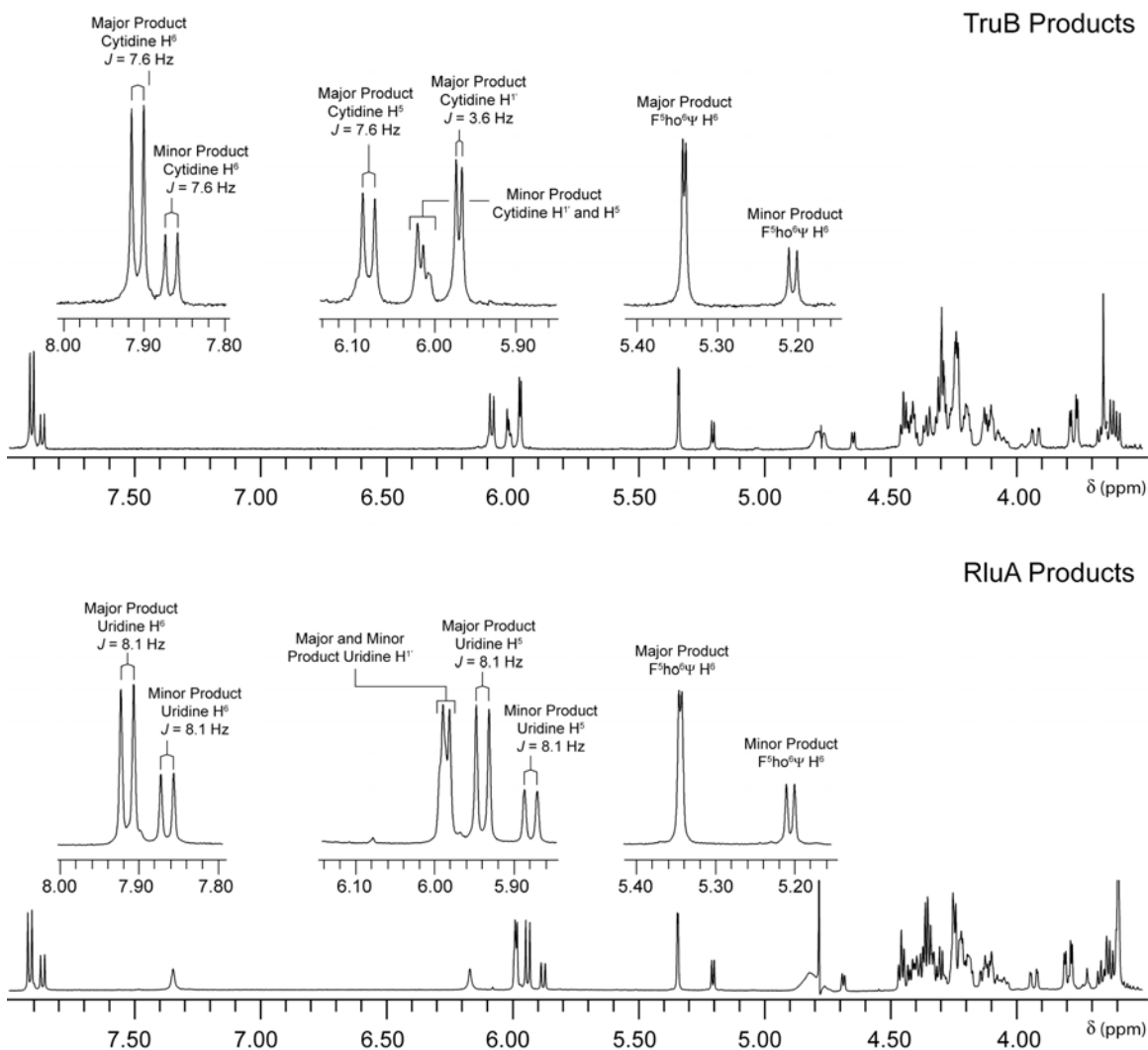


**Figure 3.** The  $^1\text{H}$  NMR spectra of the dinucleotide products of  $\text{F}^5\text{U}$  in RNA from the action of TruB (*above*) and RluA (*below*). The 3' nucleoside is either C or U, respectively, due to the difference in the sequences of the  $[\text{F}^5\text{U}]\text{RNA}$ .

*The acquisition of spectral data for the mononucleotide product(s) of  $\text{F}^5\text{U}$  resulting from the action of RluA on stem-loop  $[\text{F}^5\text{U}]\text{RNA}$  if the dinucleotide product spectra are not definitive in establishing that they are the same as from the action of TruB.*

The full suite of NMR experiments carried out on the products from RluA action, and in all cases, the results closely matched those for the products of TruB action (*e.g.*, Figure 4), which indicates that the two enzymes almost surely generate the same products of  $\text{F}^5\text{U}$  and render the need to obtain mononucleotide products from the action of RluA.

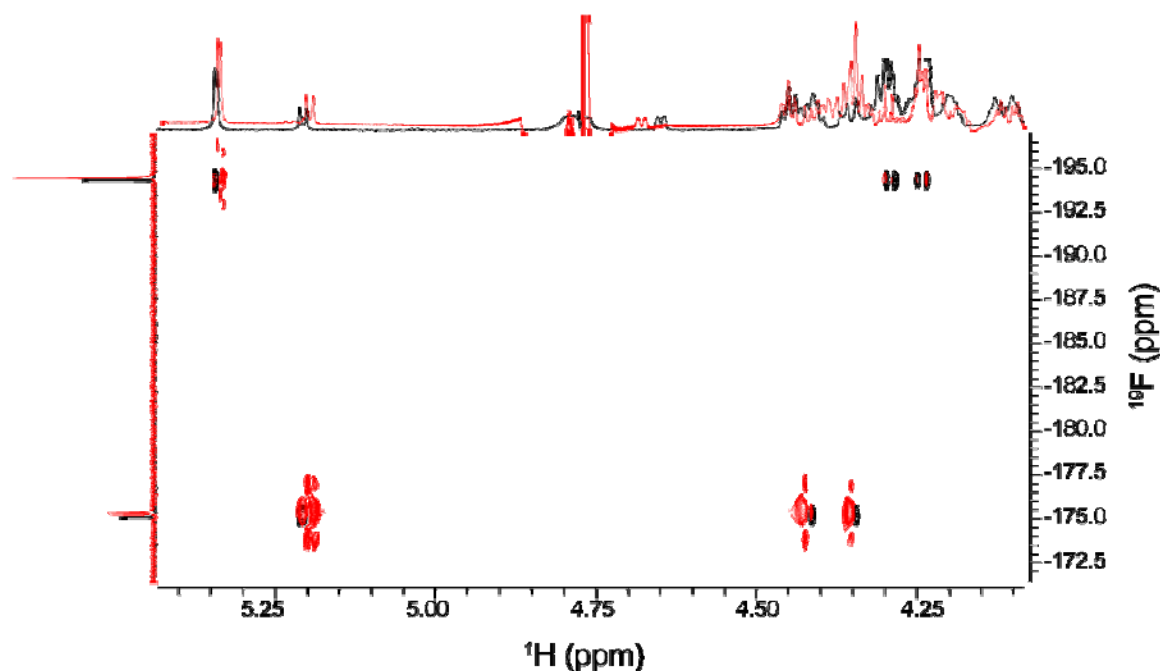


**Figure 4.** Overlay of the  $^1\text{H}$ - $^{19}\text{F}$  HSQC spectra of the dinucleotide products of  $\text{F}^5\text{U}$  in RNA from the action of TruB (*black*) and RluA (*red*).

## Task 2. Devising new nanocomposites that can enhance wound healing (Dr. M. C. Yappert).

Year 1. Synthesize magnesia nanoparticles that effectively bind ATP and other polar compounds.

a. Sequential preparation of MgO/ATP nanocomposites.

Magnesia nanoparticles were synthesized using two different approaches:

- i) Reaction of Mg acetate with NaOH, and
- ii) Reaction of Mg ethoxide with water

The ratio of water to ethanol (or isopropanol) was varied from 1:0 (water only), to 1:0.25 to 1:0.50 and 1:0.75 and 0:1 (alcohol only). The addition of the reagents was performed in a conventional bath sonicator and also using a more powerful probe sonicator. The first reaction led to more aggregation.

Dynamic light scattering (DSL) studies were performed in all of the products to measure the particle size at different times after each reaction was completed. Both DLS and visual observations indicated, for all the reactions conducted, the presence of near  $\mu\text{m}$  size particles as well as larger ( $\sim 10\text{-}\mu\text{m}$  diameter). To remove these large particles, centrifugation was performed. The fractions with the smaller nanoparticles ( $\sim 100\text{-nm}$  diameter) were collected and analyzed by infrared (IR) spectroscopy. The amount of Mg in these fractions was measured (after digestion of the particles) by atomic absorption spectroscopy. Overall, the greatest yields of the smaller nanoparticles were observed for the products of reactions performed with the aid of the probe sonicator. However, these yields were not satisfactory (5% to 6%).

The temperature at which the reactions were carried out was also varied ( $25^{\circ}\text{C}$  to  $0^{\circ}\text{C}$ ) but it did not enhance the yields of the smaller particles. Faced with these difficulties, the preparation of the MgO/ATP nanocomposites was pursued with MgO nanopowder purchased from Sigma. The surface diameter and surface area reported by Sigma-Aldrich are  $< 50\text{ nm}$  and  $130\text{ m}^2/\text{g}$  for the MgO nanopowder. The study of the interactions between the nanoparticles and ATP was performed by NMR spectroscopy and these results are going to be submitted as a manuscript during this month.

Reaction ii mentioned above was carried out in the presence of ATP in the aqueous solvent. The reaction product was allowed to settle overnight and then UV-vis and IR spectra were collected to determine the amount of ATP present in both the precipitate and the supernatant. The UV-vis traces showed a slight but reproducible shift in the absorption of ATP in the MgO/ATP nanocomposites relative to the ATP control. The presence of ATP led to a small improvement in the yield of the nanocomposites (5% to 7%), suggesting that ATP reduces the aggregation of the nanoparticles. Given the low yield of the reactions, the combined preparation of the nanohybrids, while feasible, is not going to be pursued.

B, Characterize interactions between MgO nanoparticles and ATP.

As the surface charge of metal oxide nanoparticles is affected by pH, we explored changes in  $^1\text{H}$  and  $^{31}\text{P}$  NMR chemical shifts of ATP-related resonances in aqueous solutions (pH: 4.2, 7.4 and 9.5) as the concentration of commercially available MgO nanoparticles was increased. The experimental trends indicate that the strongest interactions occur at physiological pH when the MgO nanoparticles are still positively charged and the  $\gamma$  phosphate group of ATP is undergoing its final deprotonation. Although the nanoparticles lead to the partial 'opening' of the 'self-stacked' form of ATP (at pH 7.4 and 9.5) in which the phosphates are stacked onto adenine, the major interactions with the MgO nanoparticles occur via direct attachment of the  $\alpha$  and  $\beta$  phosphates.

### **Task 3 Characterization of the complex between Factor XIII and fibrinogen (Dr. M. C. Maurer).**

Year 1. *E. coli* systems for expressing and purifying  $\alpha\text{C 242-424}$  will be optimized for producing the large amounts of isotopically labeled protein needed for NMR studies. We anticipate that both wild type and selected mutants will be desired for the studies. Unlabeled recombinant wild type FXIII A2 and human derived FXIII B2 will also be collected. Assessing NMR chemical shift assignments will begin.

Members of the coagulation cascade have far reaching effects on stemming blood loss, promoting wounding healing, and controlling heart disease, stroke, and arteriosclerosis. In the clotting process, thrombin cleaves off the N-terminal portions of the  $\text{A}\alpha$  and  $\text{B}\beta$  chains of fibrinogen ( $\text{A}\alpha\text{B}\beta\gamma_2$ ) to release FpA and FpB. The resultant fibrin monomers polymerize into ordered fibrin arrays. Activated Factor XIII (FXIII) is then responsible for catalyzing the formation of covalent crosslinks within the fibrin network and in fibrin-enzyme complexes. One of the binding sites for FXIII on fibrin has been found within  $\alpha\text{C 242-424}$ , a segment located in the C-terminal portion of the fibrinogen  $\text{A}\alpha$  chain. The main objective of the current research is to examine in solution the structural and dynamic properties that govern interactions between FXIII and Fbg  $\alpha\text{C 242-424}$ .

DNA for expressing Fbg  $\alpha\text{C 242-424}$  and FXIII A<sub>2</sub> in *E. coli* have been obtained from collaborators. Strategies for expressing and purifying the resultant proteins have been developed and primers for required mutants have been designed. These approaches will now be implemented in the coming months. It will be important to

verify that the expressed FXIII A<sub>2</sub> is active and that the Fbg αC 242-424 can serve as an effective transglutaminase substrate. A kinetic assay that utilizes MALDI-TOF mass spectrometry for detecting loss of substrate and gain of product has been optimized. For the larger substrate Fbg αC 242-424, we will need to proteolytically digest the quenched kinetic samples with chymotrypsin prior to MALDI analysis. Some of the NMR studies will involve mapping interactions between FXIII subunits and Fbg αC 242-424. Amide proton hydrogen-deuterium exchange coupled with MALDI-TOF mass spectrometry (HDX-MS) is a complementary method to probe such interactions. Moreover, HDX-MS can be very helpful for examining protein regions where NMR chemical shifts cannot be assigned. We have collected data on the conformational effects that FXIII A<sub>2</sub> undergoes in the presence of different monovalent and divalent cations. Further knowledge has thus been gained on solution environments that can activate the transglutaminase and the structural consequences. The new information being collected on these different biophysical and kinetic sub-projects may aid in the design of new therapeutic agents to control blood loss and/or wound healing.

During the past quarter, further work has been carried out on setting up the expression system for Fbg αC 242-424 in Ecoli. Lab members have been trained in the required molecular biology methods and initial stages of the research work have taken place. A system which will subsequently be used to purify the expressed protein has been established. Further progress has also been made in using HPLC methods to follow activation of intact FXIII A<sub>2</sub>. Some of the proposed NMR studies will involve mapping interactions between FXIII subunits and Fbg αC 242-424. Amide proton hydrogen-deuterium exchange coupled with MALDI-TOF mass spectrometry (HDX-MS) is a complementary method to probe such interactions. Further results have been obtained on FXIII regions that become exposed upon activation and are likely available for interactions with other proteins. Such information will become valuable for subsequent NMR studies on Fbg αC 242-424 and its responses to the introduction of FXIII A<sub>2</sub>.

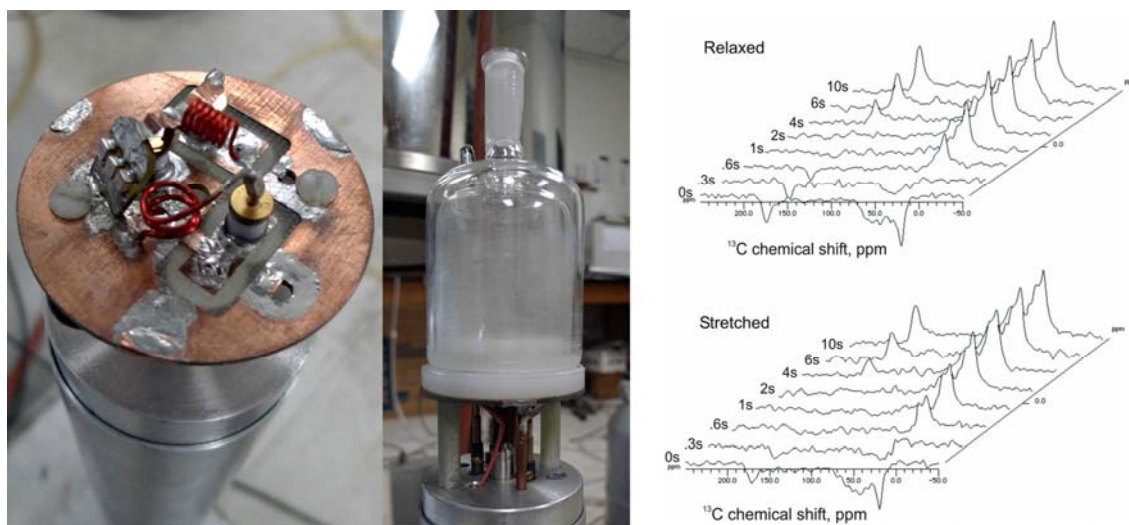
#### **Task 4**

##### **d. Tensile properties of fibrous proteins (Dr. R. J. Wittebort)**

Year 1: Complete <sup>13</sup>C, <sup>2</sup>H and <sup>17</sup>O NMR of elastin to test hypothesis I. Publish results on elastin's mechanism of elasticity. Express and purify collagen constructs.

Our year 1 milestones includes three goals: (i) complete <sup>13</sup>C, <sup>2</sup>H and <sup>17</sup>O NMR of elastin to test hypothesis I, (ii) publish results on elastin's mechanism of elasticity and to (iii) express collagen constructs. In this 3rd-quarter, year-1 report the following significant Progress toward these milestones.

Regarding (i), two probes have been constructed and tested (shown in the first two panels of figure below) for executing the <sup>13</sup>C, <sup>2</sup>H and <sup>17</sup>O NMR experiments on the 500 MHz instrument. These probes have excellent sensitivity and are adapted for variable temperature experiments (see installed sample dewar in the 2nd panel below).

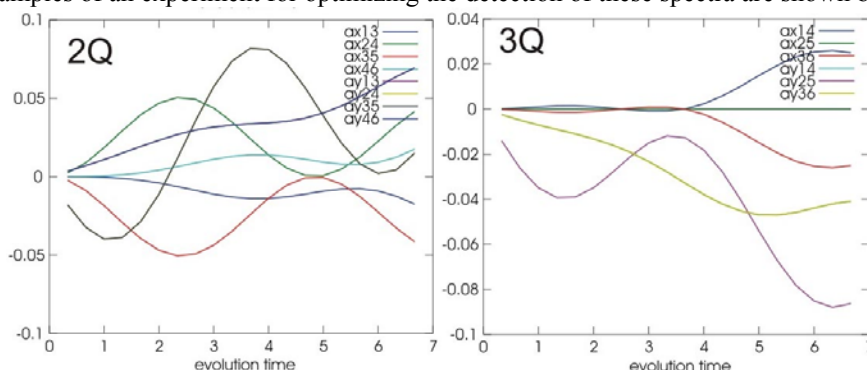


$^{13}\text{C}$  relaxation data collected from elastin using this equipment is shown in the 3rd panel and summarized below.

site	T1 Stretched sec.	Relaxed
CO	$5.3 \pm 0.8$	$4.1 \pm .4$
Ca	$1.29 \pm .22$	$1.20 \pm .14$
$\text{CH}_3$	$0.53 \pm .04$	$0.52 \pm .03$

Variable temperature  $^{17}\text{O}$  spectra of non-stretched elastic fibers equilibrated against  $\text{H}_2^{17}\text{O}$ , not shown, display significant inhomogeneous line broadening resulting from protein:solvent interactions. Together, these data show that dynamics of the elastin chain vary little with stretch, however, elastin significantly perturbs the rotational dynamics of the surface water.

The effect of inhomogeneous line broadening in the  $\text{O}^{17}$  experiments is now being investigated in detail using multiple-quantum NMR. We have developed a suite of programs to optimize and interpret results from these experiments. Examples of an experiment for optimizing the detection of these spectra are shown below.

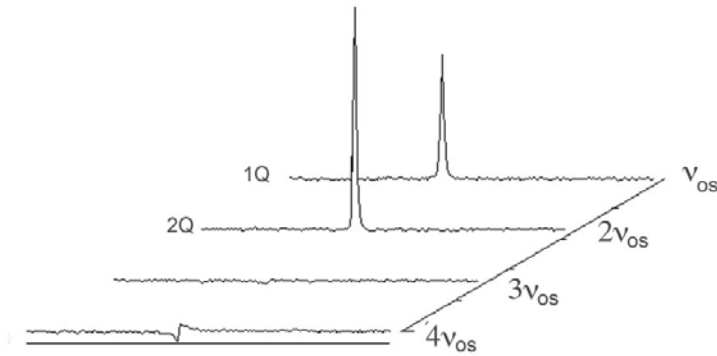


Specifically, we will measure solvent double (2Q) and triple (3Q) coherences to determine the amount of ordered water and the degree that it is ordered as a function of stretch. This, along with measurement of field-dependent  $^{13}\text{C}$  relaxation dispersion, will complete these studies for publication (goal ii). This will be done during the 4th-quarter of year-1. The latter will become possible after completion of the 700 MHz instrument installation. At the time the instrument was purchased, installation during 12/09 was promised, however, the manufacturer has imposed significant delays and completion during 8/10 seems possible.

For goal iii (expression of heterotrimeric collagen fibers) we are collaborating with Professor Ron Koder (dept. of physics, CUNY). Ron's lab has expressed 22 proteins in the past two years and previously helped us express a 46-residue collagen fragment. The plasmid genes coding these constructs are being prepared commercially and Ron's group will guide us in transforming an expression strain of *e-coli*.

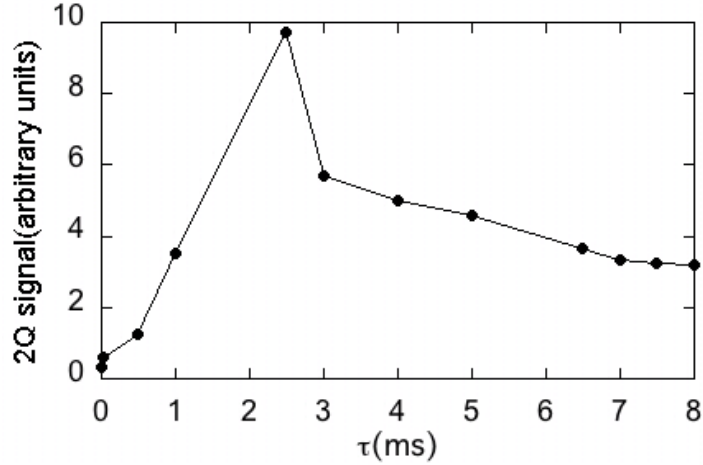
During the final quarter of year one, efforts were focused on two aspects of this project: (i) refining pulse sequences for sensitive and accurate acquisition of  $^2\text{H}$  and  $^{17}\text{O}$  double quantum spectra of elastin and (ii) design and preliminary construction of the triple resonance MAS probe.

With regard to (i), we can now collect high quality spectra that rigorously separate 2Q and 1Q signals using a combination 2Q filtration and two-dimensional (2D) separation of the 1Q and 2Q signals. High quality spectra are obtained with small elastin samples (5-10 mg) in three minutes of acquisition time. An example, collected on a fully hydrated elastin sample is shown below. Although the spectra are 2Q filtered, a small 1Q signal is still observed. In general, the 1Q:2Q signal ratio is not known and could easily be 100:1 or larger in these fully hydrated elastin samples. In our hands, 2Q filtration has a 50-fold rejection of the 1Q signal, so we devised an efficient 2-dimensional experiment that separates the residual 1Q signal from the desired 2Q signal in the indirect frequency dimension.



The experiment uses a constant time evolution period for the indirect dimension that separates the 1Q and 2Q signals on the basis of their different dependence on the offset frequency. Consequently, only 8 time increments in the indirect dimension are required to separate the 1Q signal and the entire 2Q signal appears in a signal slice. Thus, there is no S/N disadvantage relative to a 1D experiment and the 2Q signal intensity is unambiguously observed.

The DQ signal results from waters that are ordered, i.e., waters that are not isotropically reorienting and have lower entropy because of interaction with the matrix of the elastic protein. Our fundamental question is to determine to what extent does lower entropy “surface” water contribute to the entropy driven recoil of elastin. To do this, we will measure both changes in the amount of ordered water and the degree of water ordering as functions of elastin stretch and hydration. In our experiment, the amount of ordered water is proportional to the 2Q signal intensity and the degree of ordering is proportional to the residual quadrupole coupling,  $\bar{\omega}_q$ . The coupling is determined from the t-dependence of the 2Q signal intensity,  $\sin(\bar{\omega}_q \tau) e^{-\tau/T_{2,2Q}}$ , in the 2Q preparation period of the 2D experiment. This t-dependence is shown in the graph below.



The pulse sequence also allows us to independently measure  $T_{2,2Q}$ . Thus, determining  $\bar{\omega}_q$  from the above data amounts to a single parameter fit. Preliminary inspection of the data indicates that  $\bar{\omega}_q / 2\pi \approx 100$  Hz.

In the next quarter, our probe and pulse sequence will allow us to make extensive measurements on the stretch and hydration dependence of water ordering in elastin. We expect that our approach is unique with regard to sensitivity, the ability to rigorously eliminate interference from 1Q signals and the use of NMR signals from both  $^2\text{H}_2\text{O}$  and  $\text{H}_2^{17}\text{O}$ .

Regarding (ii), construction of the  $1\text{H}/^{13}\text{C}/^{15}\text{N}$  triple resonance probe, an undergraduate honors student worked productively over the summer. He derived relevant design equation for the RF circuit, bread boarded the circuit, modified our probe tuning instrument for operation at 700 MHz, and confirmed that the design circuit can be tuned to the three NMR frequencies. Design equations are summarized in the table below.

Description	Nucleus	Tune	Match
Parallel resonant, Series $C_m$ Match	$^{13}\text{C}/^{15}\text{N}$	$\omega^2 L = \frac{1}{(C_m + C_t)}$	$\frac{1}{\omega C_m} = \frac{Z_o \omega L}{R}$
Series Resonant, Parallel $C_m$ Match	$^1\text{H}$	$\omega^2 L = \frac{1}{C_t} + \frac{1}{C_m}$	$\frac{1}{\omega C_m} = \sqrt{R Z_o}$
Series Resonant, Parallel $L_m$ Match	$^1\text{H}$	$\omega^2 (L_m + L) = \frac{1}{C_t}$	$\omega L_m = \sqrt{R Z_o}$

In the above,  $L$  and  $C_t$  are the sample inductor and resonant capacitor, respectively. Subsequently, the student produced compact circuit boards for testing the probe in the 700 MHz magnet and is now preparing the complete mechanical design which contains a novel and more accurate mechanical apparatus for adjusting the magic angle. Overall, the probe is a triple resonance implementation of the highly efficient circuit used in the elastin studies. Consequently, we expect it to be similarly effective.

## **KEY RESEARCH ACCOMPLISHMENTS:**

Task 1. We overexpressed the active C-terminal domain of enzyme ThiI, required for 4-thiouridine modification of tRNA. The two pseudouridine synthetases, TruB and RluA convert uridine to pseudourine in tRNA. We show the two enzymes generate the same products of F<sup>5</sup>U.

Task 2. Nanoparticles of MgO were synthesized and their interactions with ATP were characterized.

Task 3. Set up an expression system for Fbg  $\alpha$ C 242-424 in Ecoli. A protocol for purification has been determined.

Task 4. NMR probes for elastin spectroscopy built and tested. An expression system for heterodimeric collagen has been established. The entropy of water molecules on the surface of elastin has been measured.

## REPORTABLE OUTCOMES:

### Research

Jadhav, MA; Isetti, G; Trumbo, TA, and Maurer, M.C. Effects of Introducing Fibrinogen A alpha Character into the Factor XIII Activation Peptide Segment *Biochemistry*, **49**: 2918-2924 (2010).

Nyunt, MT; Dicus, CW; Cui, YY, Yappert, MC, Huser, TR, Nantz, MN and Wu, J.  
Physico-Chemical Characterization of Poly lipid Nanoparticles for Gene Delivery to the Liver  
*Bioconj. Chem.*: **20**, 2047-2054 (2009).

### *Presentations*

### *Patents*

none

## Conclusions

During the period covered by this report, a Request for Proposals was issued for instrumentation that was required for the successful conduct of the research described. The bids from Bruker and Varian were analyzed and it was decided to purchase a 400 MHz NMR, a 700 MHz NMR and a small-molecule x-ray diffractometer from Varian. These were installed and tested have recently become fully operational. In a parallel effort, the four research labs have been working toward the goal of utilizing these instruments for their specific projects. For Task 1, led by Professor Mueller, the active C-terminal domain of enzyme ThiI, required for 4-thiouridine modification of tRNA was overexpressed and can be prepared for NMR data acquisition. The two mononucleotide products of F<sup>5</sup>U obtained from the action of TruB will now be rerun on the 700 MHz NMR to strengthen the conclusion that the two products are constrained conformers. For Task 2, led by Professor Yappert, characterization of the synthesized MgO nanoparticle interaction with ATP has been accomplished by NMR, indicating a direct interaction. This is important if these compounds are to be useful in wound healing. Task 3, led by Professor Maurer, has developed the expression systems for the relevant portions of Factor XIII and fibrinogen and, with the spectrometers in place, characterization of this key interaction in the blood clotting cascade can be elucidated. Task 4, led by Professor Wittebort, saw the expression of heterodimeric collagen fibers and an expression system for a 46-residue collagen fragment is being readied. Concurrently, two NMR solid-state probes have been constructed and NMR studies are being performed to show the degree of water structuring as a driving for the tensile strength and elasticity of these fibers.

## References

- Jadhav, MA; Isetti, G; Trumbo, TA, and Maurer, M.C. Effects of Introducing Fibrinogen A alpha Character into the Factor XIII Activation Peptide Segment *Biochemistry*, **49**: 2918-2924 (2010).
- Marley, J., Lu, M and Bracken, C. *J. Biomol. NMR*, **20**, 71-75 (2001).
- Nyunt, MT; Dicus, CW; Cui, YY, Yappert, MC, Huser, TR, Nantz, MN and Wu, J.  
Physico-Chemical Characterization of Poly lipid Nanoparticles for Gene Delivery to the Liver  
*Bioconj. Chem.*: **20**, 2047-2054 (2009).

